Thermochimica Acta, 86 (1985) 45–58
Elsevier Science Publishers B.V., Amsterdam – Printed in The Netherlands

THERMOANALYTICAL INVESTIGATION OF HUNTITE

R. OZAO * and R. OTSUKA

Department of Mineral Industry, School of Science and Engineering, Waseda University, 3-4-1, Okubo, Shinjuku-ku, Tokyo (Japan)

(Received 25 September 1984)

ABSTRACT

This work investigates the thermal decomposition of huntite, $CaMg_3(CO_3)_4$, comparing it to that of dolomite. A small amount of the sample (5.0 mg) is used under atmospheres of various CO_2 partial pressures.

In the CO_2 atmosphere, huntite decomposes in two steps

$$CaMg_3(CO_3)_4 \rightarrow \underset{\text{(Mg–calcite)}}{CaCO_3 \cdot n MgCO_3} + (3-n)MgO + (3-n)CO_2 \quad \text{(i)}$$

(n gradually changes with increasing temperature from 0.2 to 0.05).

$$CaCO_3 \cdot n MgCO_3 \rightarrow n MgO + CaO + (1+n)CO_2 \quad \text{(ii)}$$

($n \leqslant 0.05$)

It has been clarified that both decompositions are straightforward dissociations similar to those of magnesite and calcite, and that their decomposition temperatures shift towards the higher temperature side with increasing CO_2 partial pressure.

Therefore, it may be concluded that the mechanism of the first decomposition of huntite is quite different to that of dolomite.

INTRODUCTION

Huntite, $CaMg_3(CO_3)_4$, is a mineral of rare occurrence in nature. It was first described by Faust [1]. The crystal structure of huntite was determined by Graf and Bradley [2]. They indicated that it is an ordered double carbonate similar to dolomite.

Regarding the thermal properties of huntite, the heat capacity was measured from 18 to above 306 K by Hemingway and Robie [3]. DTA curves were obtained by several workers [1,4–7]. They recognized that huntite is characterized by two distinct endothermic peaks at 600–650°C and ~ 900°C, representing the decomposition of the magnesium carbonate portion and the calcium carbonate portion, respectively. A detailed study of the thermal

* Present address: Institute of Earth Science, Waseda University, 1-6-1, Nishiwaseda, Shinjuku-ku, Tokyo, Japan.

0040-6031/85/$03.30

decomposition of huntite, however, has not yet been carried out. Therefore, in the present study, as a part of the thermoanalytical investigation of dolomite and related minerals [8,9], the thermal decomposition of huntite was studied in detail in comparison with that of dolomite.

MATERIAL

Huntite from Tea Tree Gully, South Australia was used in this study. It is massive and white with a chalky appearance. Microscopic observation revealed that it consisted of minute grains of $< 1-2$ μm in diameter. X-ray powder analysis showed no phases other than huntite. Lattice parameters obtained by X-ray powder diffraction using silicon (NBS standard material SRM 640) as an internal standard were: $a = 9.505 \pm 0.001$ and $c = 7.815 \pm 0.002$ Å, which are in good agreement with those calculated by Graf and Bradley [2] (JCPDS card No. 14-409). The results of a chemical analysis of the present sample obtained by EPMA are given in Table 1, together with those of another three samples from the same locality given in the literature.

EXPERIMENTAL

Huntite was ground in an agate mortar and then sieved to obtain fractions in the range of 39–43 μm.

TABLE 1

Chemical composition of huntite from Tea Tree Gully, South Australia

	wt%			mol%	
	1	2	3	4	4′
MgO	33.4	34.4	33.2	33.71	76.10($MgCO_3$)
CaO	15.3	16.0	15.6	14.70	23.80($CaCo_3$)
MnO	–	–	–	0.03	0.00($MnCO_3$)
FeO	–	–	–	0.05	0.01($FeCO_3$)
CO_2	48.5	50.4	48.9	48.39	
SiO_2	0.08				
$H_2O(-)$	0.16				
$H_2O(+)$	1.4				
Na_2O	0.22				
Total	99.06	100.8	97.7	96.88	

1 Hemingway and Robie [3].
2,3 Skinner [10].
4 Present study: analyzed by JEOL JXA 733 electron microprobe analyzer. Correction was made by the method of Bence and Albee.
4′ Present study: expressed in cation mole ratio (mol%).

DTA measurement

Measurements were performed under the following atmospheric conditions, using a Rigaku Thermoflex TG–DTA, on 5.0 mg of sample at the programmed heating rate of 10°C min^{-1}.

(1) CO_2 flow of 100 ml min^{-1}.

(2) Mixed gas flow of CO_2 and N_2, varying their mixing ratios, where the total flow was maintained at the constant rate of 100 ml min^{-1}.

X-ray powder analysis

The phase identification of reaction products was made by X-ray powder analysis using a Rigaku RAD I under the following conditions: graphite-monochromized Cu $K\alpha$ radiation; 40 kV–20 mA; time constant, 2 s; scanning speed, 0.5° min^{-1}; divergence slit, 1°; receiving slit, 0.3 mm; and scattering slit, 1°. Samples heated to specified temperatures were quickly cooled down to room temperature by removing the furnace for phase identification.

Infrared absorption analysis

Each 1.5-mg sample of the reaction product and 200 mg of KBr were pressed into 13 mm diameter disks, and absorption spectra were recorded using a Hitachi 260-50 infrared spectrophotometer.

TEM observation

The above reaction products were also subjected to TEM observation using a Hitachi transmission electron microscope H-500H at the accelerated voltage of 100 kV.

RESULTS

DTA curves

Figure 1 shows the DTA curves of huntite and related carbonates recorded under a CO_2 gas flow of 100 ml min^{-1}. Huntite showed two endotherms in a similar manner to dolomite, however, their temperature ranges, peak profiles and peak areas were completely different. The first endotherm (abbreviated to 1st En in this text) of dolomite appeared at a higher temperature (T_e = 714°C) than the decomposition temperature of magnesite (T_e = 617°C), whereas that of huntite was recognized at a lower temperature (T_e = 594°C). In addition, huntite yielded a magnesite-like, sharp and symmetric peak differing from that of dolomite.

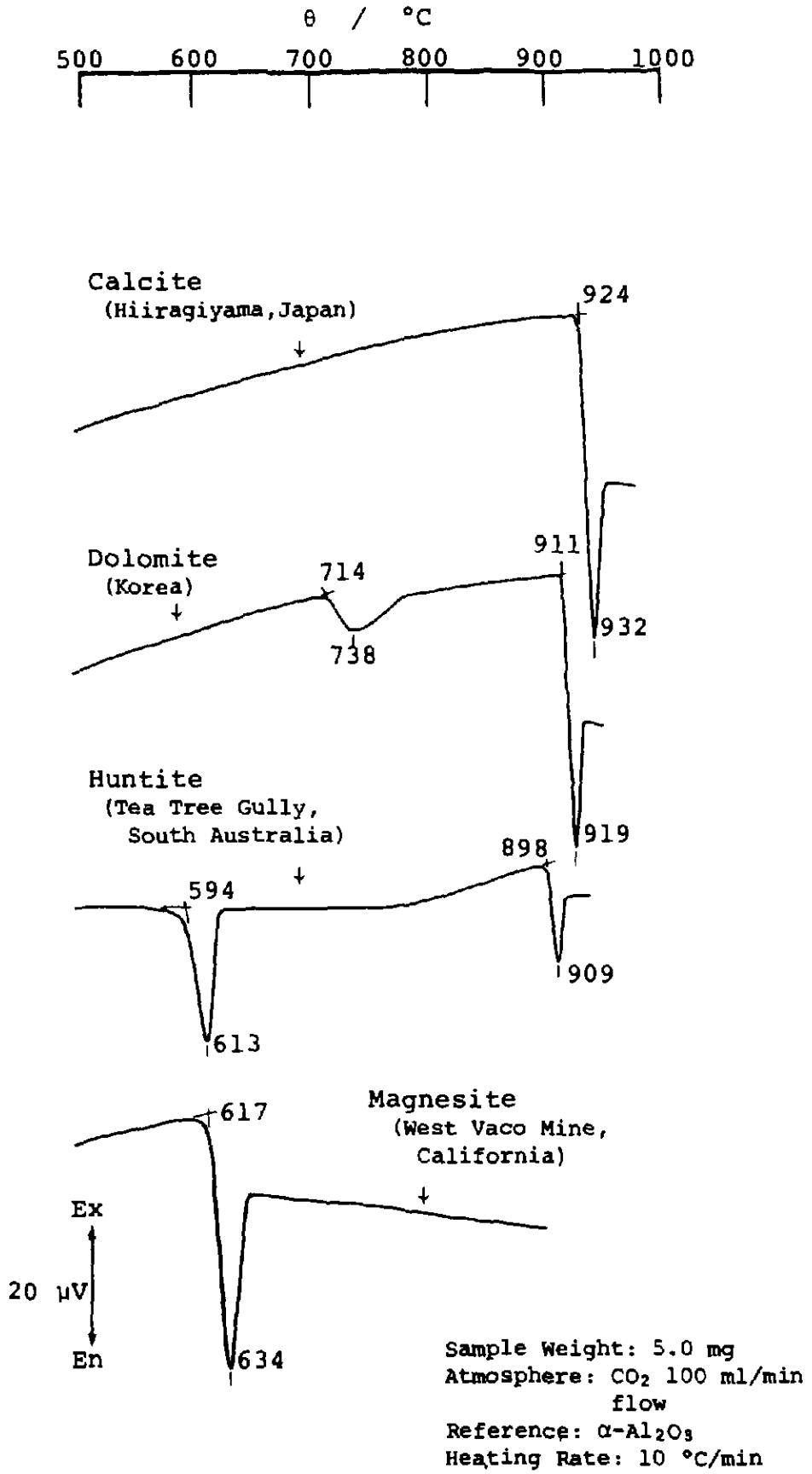

Fig. 1. DTA curves of huntite and related carbonates.

A similar tendency was observed on the second endotherm (2nd En); its temperature range decreased in the order: calcite ($T_e = 924°C$) > dolomite (911°C) > huntite (898°C).

The baseline of huntite suddenly shifted to the exothermic side in the range 750–800°C after the 1st En terminated, whereas those of calcite and dolomite gradually shifted to the exothermic side with heating.

Figure 2 compares the DTA curve of (a) 3:1 (mole ratio) mechanical mixture of magnesite and calcite, with that of (b) huntite. Peak temperatures and peak profiles of curve (a) were characteristic to the component minerals (magnesite and calcite), and clearly differed from those of curve (b).

Figure 3 shows DTA curves obtained in the mixed gas flow under various mixing ratios of CO_2 and N_2. Both the 1st and 2nd Ens broadened and shifted to the lower temperature side with decrease in CO_2 partial pressure, however, the shift of the 1st En was not as sensitive as the 2nd En. The shift in the range of CO_2 from 100 to 0% was equal to about 70° for the 1st En, whereas that for the 2nd En was as large as 250°.

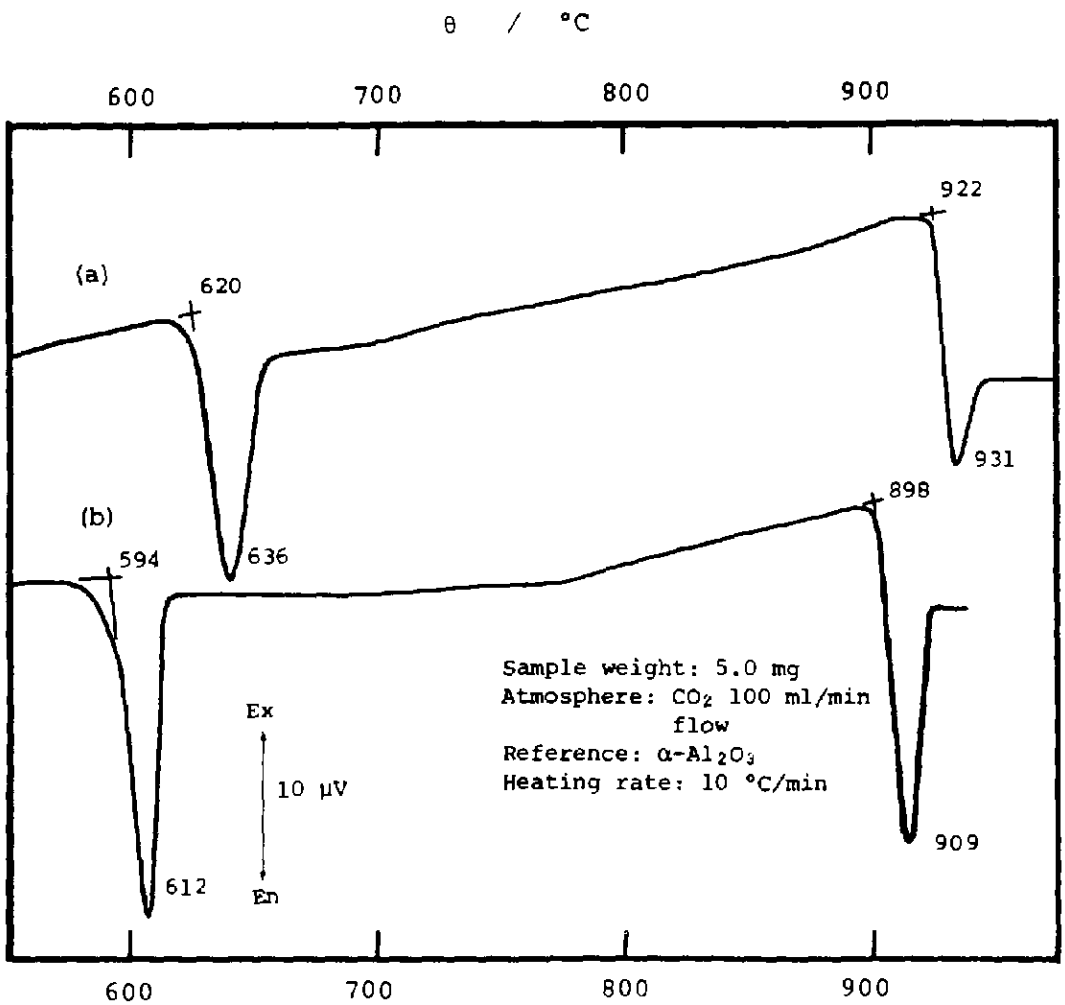

Fig. 2. DTA curves of: (a) mechanical mixture of magnesite and calcite ($MgCO_3 : CaCO_3$ = 3:1) and (b) huntite (particle size −325/400 mesh).

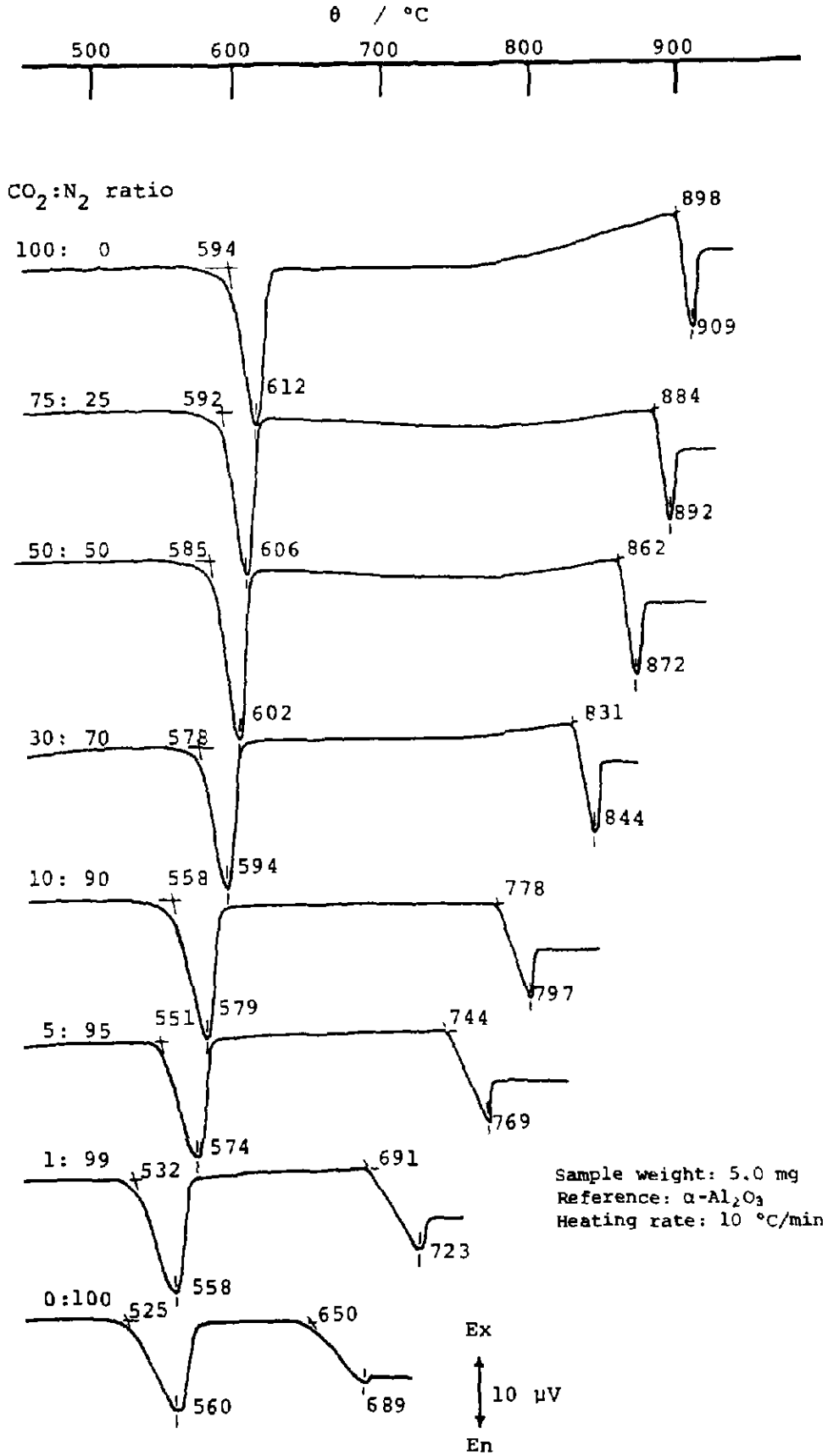

Fig. 3. DTA curves of huntite under mixing gas flow of CO_2 and N_2. Total gas flow rate is 100 ml min^{-1}.

Identification of products

X-ray diffraction patterns and IR absorption spectra of the products obtained at each specified temperature are given in Fig. 4.

At 573°C

All other X-ray peaks, except a broad peak attributed to periclase (marked with p in the figure), are identified as huntite. Similarly, an IR spectrum characteristic to huntite was obtained. Two split absorption bands at 1530 and 1440 cm^{-1}, and 858 and 880 cm^{-1} are due to the ν_3 and ν_2 vibrations, respectively, of crystallographically different CO_3 groups, which are characteristic to huntite. The 1110 and 742 cm^{-1} bands are assigned to the ν_1 and ν_4 vibrations, respectively (Scheetz and White [11]).

At 619°C

The reaction products obtained immediately after the 1st En were poorly crystallized MgO and a calcite-like phase. The reflections of the latter shifted to the higher-angle side. The calculated lattice constants from these reflec-

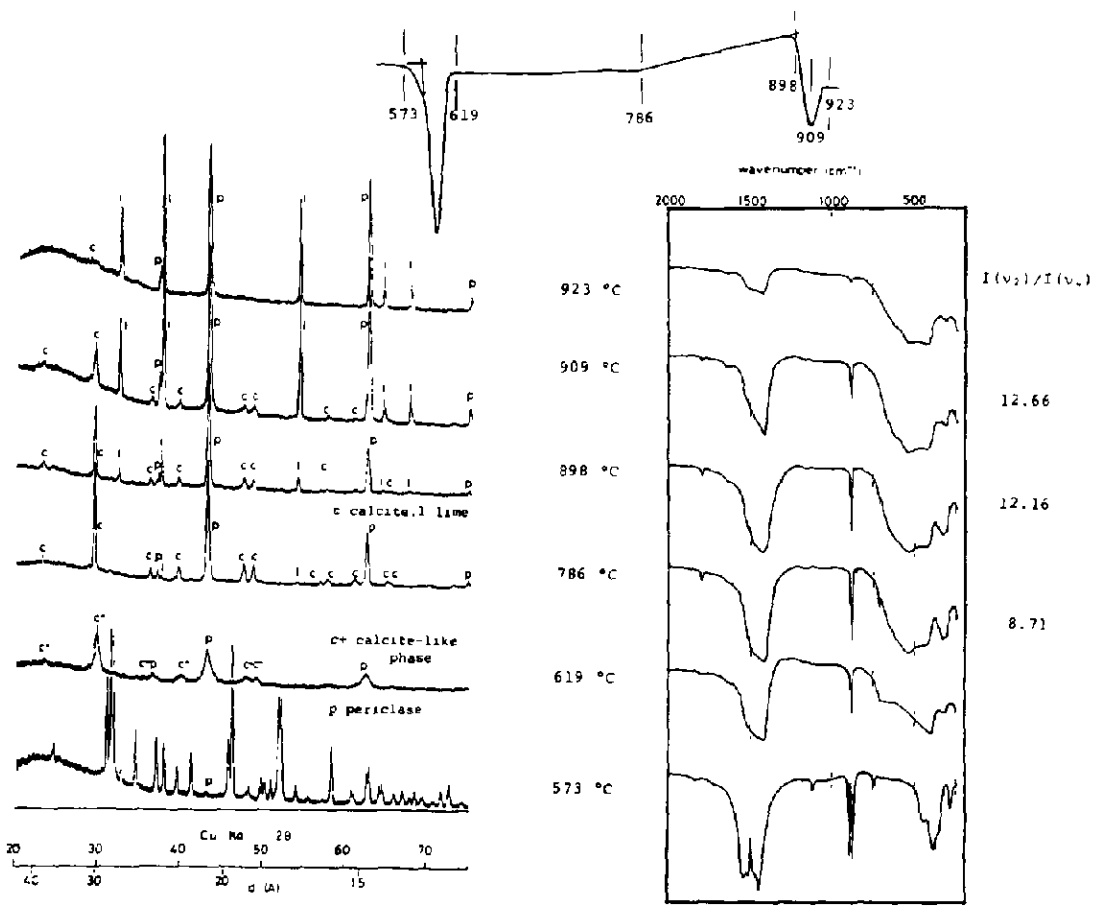

Fig. 4. Identification of products at various temperatures by X-ray and IR analyses.

tions were: $a = 4.91$ and $c = 16.99$ Å, which were rather small, compared to those of normal calcite ($a = 4.99$, $c = 17.05$ Å).

Similarly, the ν_2 and ν_3 split bands characteristic to huntite completely disappeared. The ν_2 and ν_4 bands characteristic to a calcite structure should appear at 880 and 712 cm^{-1}. However, the ν_4 absorption band was not clearly separated, suggesting that the product is not normal calcite but a calcite-like phase.

At 786°C

The X-ray patterns showed the existence of calcite ($a = 4.98$, $c = 17.13$ Å), well-crystallized MgO, and a small amount of CaO. The ν_2 and ν_4 bands of of calcite were clearly recognized. The integrated intensity ratio of ν_2 to ν_4, $I(\nu_2)/I(\nu_4)$, was 8.71. This ratio represents the degree of order in the structure, and it is higher for well-crystallized than for disordered calcite [12].

At 898°C

Calcite ($a = 4.97$, $c = 17.11$ Å), MgO and CaO were recognized. The amount of CaO clearly increased. The abrupt increase in the $I(\nu_2)/I(\nu_4)$ value to 12.16 indicates the rapid increase in crystallinity of calcite.

At 909°C

Calcite ($a = 4.98$, $c = 17.11$ Å) reflections were rather attenuated in contrast to the increase in intensities of CaO reflections, suggesting the decomposition of calcite. Intensities of MgO reflections also increased.

At 923°C

Calcite was almost completely decomposed. Very sharp reflections of CaO and MgO were recognized.

Figure 5 compares the detailed X-ray profiles of huntite and dolomite. The 104 and 202 reflections (marked with c104 and c202 in the figure) of calcite, and the 200 reflection (p200) of MgO were recorded immediately after the 1st En (marked with 1st in the figure) and just before the 2nd En (2nd).

Dolomite yielded sharp calcite reflections of c104 and c202, and a broad MgO reflection of p200 immediately after the 1st En, whereas huntite produced broad and weak reflections (c104 and c202) of calcite, respectively. Moreover, in the case of dolomite, c104 and c202 reflections reduced their intensities just before the 2nd En, in contrast to the increase in intensity of the p200 reflection. In the case of huntite, however, both the calcite and MgO reflections became sharper just before the 2nd En. In addition, in the former case (dolomite), the c104 reflection slightly shifted from 2θ(Cu

$K\alpha) = 29.50°$ to 29.42°, whereas in the latter case (huntite) the reflection moved considerably from 29.80° to 29.50°.

Hashimoto et al. [13] decomposed dolomite isothermally and observed relatively large calcite crystallites (700–800 Å in diameter) and fine MgO particles (~ 300 Å). They also reported that MgO crystallites noticeably grew with time up to 700–900 Å, but that calcite crystallites remained at their initial sizes. The present data shown in Fig. 5 strongly support these results.

In the case of huntite, it was suggested that fine crystallites of both calcite and MgO obtained after the 1st En grew with time.

In order to confirm this suggestion, bright-field TEM observations were applied to the reaction products. Figure 6 shows the micrograph of the product obtained just before the 2nd En of huntite. A round, well-developed MgO single crystal of 500–600 Å in diameter with fringes of equal thickness is marked (A) on the photograph. The diffraction image of this single crystal exhibited distinct Kikuchi patterns, which was indicative of a thick, well-developed crystal. (B) is a well-developed crystal of calcite, showing distinct rhombohedral morphology.

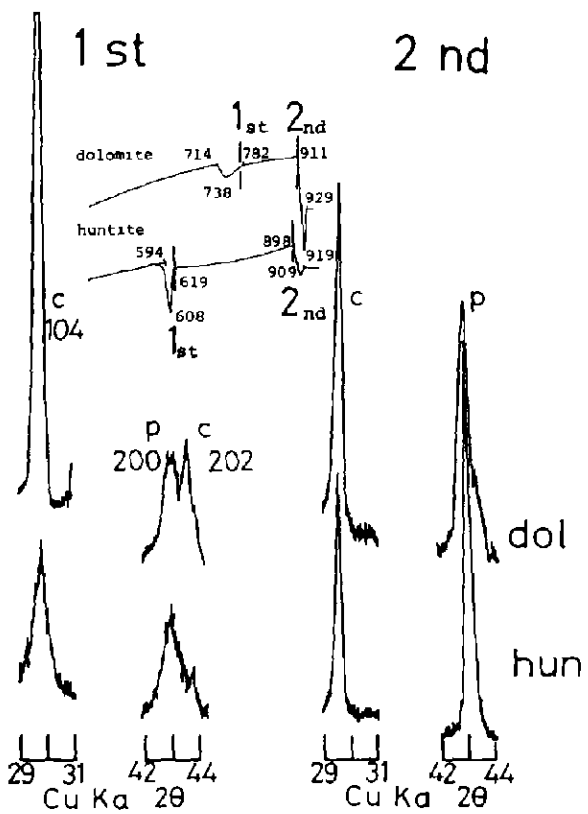

Fig. 5. Comparison of X-ray patterns of dolomite and huntite. Intensity changes of c(104), p(200), c(202) are shown. c, calcite; p, periclase.

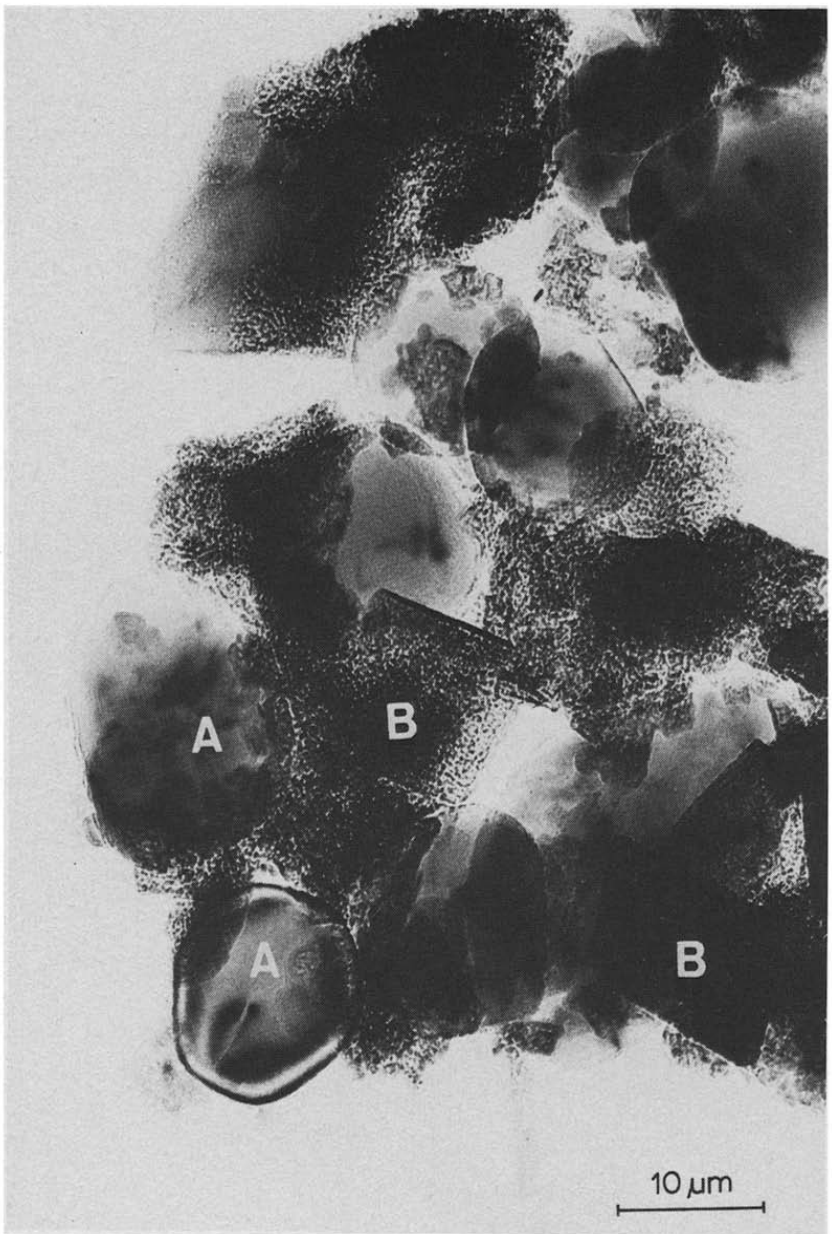

Fig. 6. Electron micrograph of the products obtained just before the 2nd endotherm of huntite.

DISCUSSION

Decomposition of huntite in CO_2

Figure 7 summarizes the results obtained from the products in Fig. 4.

(1) At 619°C, immediately after the 1st En, the decomposition products were MgO and magnesian calcite (denoted by Mg–calcite hereafter) containing approx. 20 mol% $MgCO_3$. The $MgCO_3$ content was determined from the lattice constant a using the diagram given by Goldsmith et al. [14].

(2) The above Mg–calcite gradually released Mg up to 5 mol% $MgCO_3$ at about 790°C.

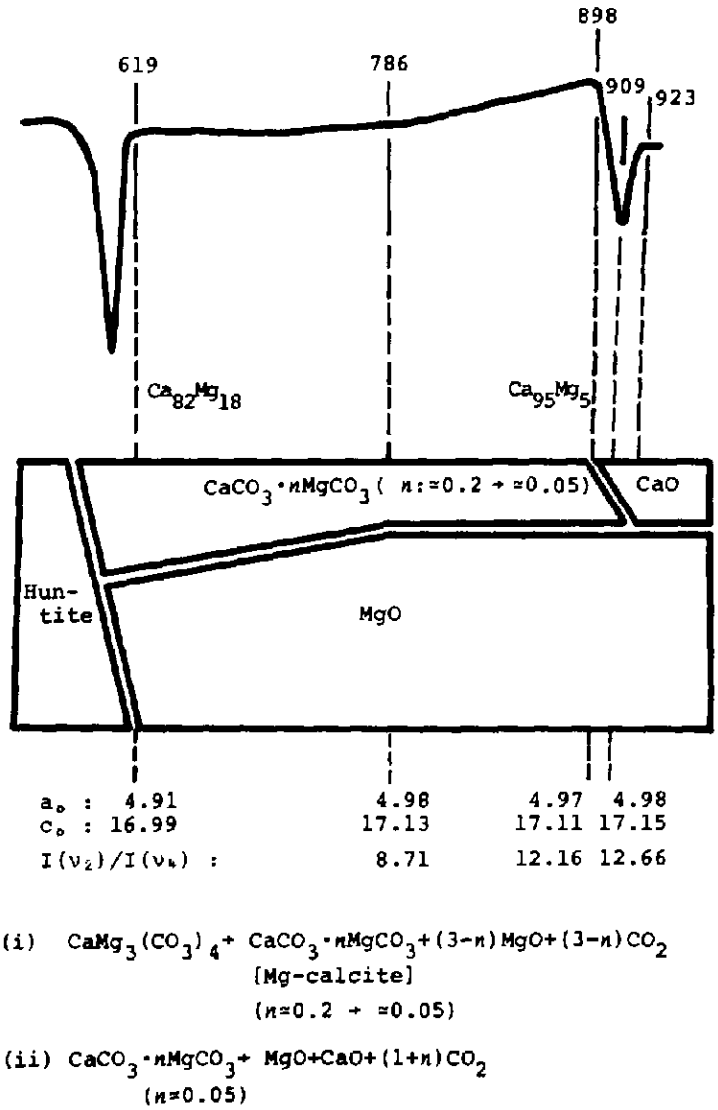

Fig. 7. Decomposition process of huntite under CO_2 flow of 100 ml min^{-1}.

(3) The $MgCO_3$ content in Mg-calcite was kept constant until 898°C, just before the 2nd En.

(4) The 2nd En was caused by the decomposition of Mg–calcite.

Therefore, it is considered that huntite decomposes in the CO_2 atmosphere in the following two steps

$$CaMg_3(CO_3)_4 \rightarrow \underset{\text{(Mg–calcite)}}{CaCO_3 \cdot nMgCO_3} + (3-n)MgO + (3-n)CO_2 \quad \text{(i)}$$

(n gradually changes with increasing temperature from 0.2 to 0.05)

$$CaCO_3 \cdot nMgCO_3 \rightarrow nMgO + CaO + (1+n)CO_2 \quad \text{(ii)}$$

($n \leqslant 0.05$)

CO_2 pressure dependence of decomposition

In Fig. 8 are plotted T_e values of the 1st and 2nd Ens of huntite given in Fig. 3 (marked with (h_1) and (h_2)) against temperature, together with those

of magnesite (m) reported by Iwafuchi [15].

The equilibrium CO_2 partial pressure vs. temperature curves for the following reactions are also given in this figure

$$CaMg_3(CO_3)_4 \rightleftarrows CaCO_3 + 3MgO + 3CO_2 \quad \text{(i)}$$

$$CaCO_3 \rightleftarrows CaO + CO_2 \quad \text{(ii)}$$

$$MgCO_3 \rightleftarrows MgO + CO_2 \quad \text{(iii)}$$

The thermodynamic properties of huntite at 298.15 K are given in Geological Survey Bulletin 1452 (1979) by Robie et al. [16]. In addition, according to Hemingway and Robie [3], above 105 K the heat capacity of huntite is equal to the sum C_p^0(calcite) + $3C_p^0$(magnesite), within 2%. In the absence of heat capacity measurements above 305 K, the additive approxi-

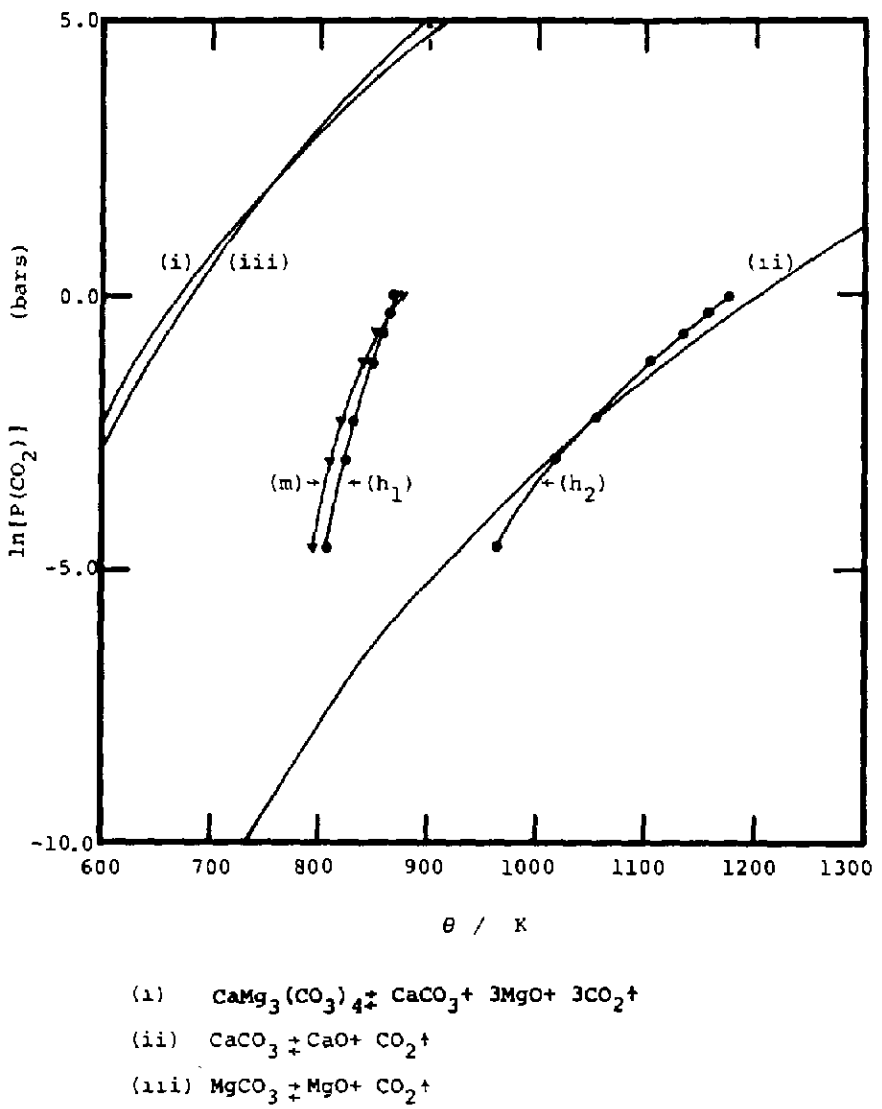

Fig. 8. Plots of T_e obtained in mixing gas flow of CO_2 and N_2. (h_1) and (h_2), 1st and 2nd endotherms of huntite; (m), magnesite (data taken from Iwafuchi [15]). Equilibrium CO_2 partial pressure vs. temperature curves are also shown.

mation should be accurate to better than 5%. Thus, the heat capacity of huntite at temperatures higher than 305 K could be expressed as:

$$C_p^0(\text{huntite}) = C_p^0(\text{calcite}) + 3 \times C_p^0(\text{magnesite})$$
$$= 343.072 + 18.368 \times 10^{-2}T - 7.654 \times 10^6 T^{-2} (\text{J mol}^{-1}\text{K}^{-1})$$

Thermodynamic properties of other materials were all obtained from the above Geological Survey Bulletin 1452 (1979).

It is clearly shown in Fig. 8 that the plots of T_e of the 2nd En of huntite agree well with the equilibrium CO_2 partial pressure vs. temperature curve of calcite. This indicates that the decomposition temperature of the calcite phase formed from the partial decomposition of huntite is very sensitive to CO_2 and it dissociates in a straightforward manner. It is well accepted that the decomposition of dolomite takes place:

(i) at high CO_2 partial pressure, in two steps

$$CaMg(CO_3)_2 \rightarrow MgO + CaCO_3 + CO_2 \rightarrow MgO + CaO + 2CO_2$$

(ii) at low CO_2 partial pressure, in one step

$$CaMg(CO_3)_2 \rightarrow MgO + CaO + 2CO_2$$

The plots of T_e of the 1st En of huntite agree quite well with those of the endotherm of magnesite. The decomposition temperatures of both huntite and magnesite decrease clearly with decreasing CO_2 partial pressure. The plots of T_e of both materials, however, deviate considerably from their equilibrium CO_2 partial pressure vs. temperature curves, indicating that the decomposition of both materials proceeds in a region where they are thermodynamically unstable. This is because the decomposition rate of magnesite is extremely slow, so that the pressure of evolved CO_2 makes it difficult to attain the equilibrium state in such a dynamic condition of heating as DTA.

It is widely recognized that the 1st endotherm of dolomite is relatively invariable with the CO_2 partial pressure of the atmosphere. Recent detailed studies [8,17,18], however, confirmed that this endotherm shifts distinctly towards the lower-temperature side with increasing CO_2 partial pressure. Therefore, CO_2 pressure affects the first decomposition temperatures of dolomite and huntite, but in opposite directions. Thus, it is clearly understood that the mechanism of the first decomposition of huntite is quite different from that of dolomite, and that it is very similar to that of magnesite.

ACKNOWLEDGMENTS

We thank Dr. S. Higuchi for the aid with TEM observations. We are also indebted to Prof. S. Tsutsumi, who kindly permitted the use of the IR spectrometer.

REFERENCES

1 G.T. Faust, Am. Mineral., 38 (1953) 4.
2 D.L. Graf and W.F. Bradley, Acta Crystallogr., 15 (1962) 238.
3 B.S. Hemingway and R.A. Robie, Am. Mineral., 57 (1972) 1754.
4 G. Baron, S. Caillere, R. Lagrange and T. Pobeguin, C.R. Acad. Sci. Paris, 245 (1957) 92.
5 A. Danilova, Zap. Tadzh. Otd. Vses. Mineral. Ova., 1 (1959) 77.
6 K. Padera and P. Povondra, Acta Univ. Carol. Geol., 1 (1964) 15.
7 D.N. Todor, Thermal Analysis of Minerals, Abacus Press, Tunbridge Wells, U.K., 1976.
8 R. Otsuka, S. Tanabe and K. Iwafuchi, Nippon Kogyo Kaishi, 96 (1980) 581.
9 K. Iwafuchi, C. Watanabe and R. Otsuka, Thermochim. Acta, 60 (1983) 361.
10 B.J. Skinner, Am. Mineral., 43 (1958) 159.
11 B.E. Scheetz and W.B. White, Am. Mineral., 62 (1977) 36.
12 H. Schneider, Mineral. Mag., 40 (1976) 314.
13 H. Hashimoto, E. Komaki, F. Hayashi and T. Uematsu, J. Solid State Chem., 33 (1980) 181.
14 J.R. Goldsmith, D.L. Graf and H.C. Heard, Am. Mineral., 46 (1961) 453.
15 K. Iwafuchi, M.Sc. Thesis, Waseda University, 1979.
16 R.A. Robie, B.S. Hemingway and J.R. Fisher, U.S., Geol. Surv., Bull. 1452 (1979).
17 W.R. Bandi and G. Krapf, Thermochim. Acta, 14 (1976) 221.
18 H. Hashimoto, Gypsum Lime, 146 (1977) 33.